Electrochromic Properties of NiO$_x$ Films Deposited by DC Magnetron Sputtering

Jianhua Qiu[1,2,*], Zhao Chen[1], Tianxiang Zhao[1], Zhihui Chen[1], Wenjing Chu[3],
Ningyi Yuan[1], and Jianning Ding[1,2]

[1]*School of Mathematics and Physics, Jiangsu Province Cultivation Base for State Key Laboratory of
Photovoltaic Science and Technology, Jiangsu Collaborative Innovation Center of Photovolatic Science and Engineering,
Changzhou University, Changzhou 213164, Jiangsu, China*
[2]*School of Mechanical Engineering, Jiangsu University, Zhenjiang 212013, Jiangsu, China*
[3]*Provincial Photoelectric Glass Key Laboratory, Changzhou Almaden Co., Ltd., Changzhou 213000, Jiangsu, China*

Nickel oxide (NiO$_x$) films were deposited onto ITO-coated glass at room temperature by DC magnetron sputtering and the electrochromic properties were investigated. The effects of film thickness on structure, morphology, electrochemical and electrochromic properties of NiO$_x$ films were systematically studied. X-ray diffraction and scanning electron microscopy results indicate NiO$_x$ films have the polycrystalline structure and the crystallinity improves with the increase of thickness. In atomic force microscopy analysis, the surface roughness of NiO$_x$ films increases as the thickness increases and large roughness is obtained in the films of more than 300 nm. The electrochemical properties were measured by using conventional three-electrode configuration in 1 M LiClO$_4$-PC electrolyte and all the samples show good cyclic stability. A transmittance modulation of 62% between colored and bleached state at 550 nm wavelength is obtained for 500 nm thick film and the high color efficiencies of more than 62 cm^{2}C^{-1} are obtained in NiO$_x$ films. However, coloring and bleaching response times increase with the increase of thickness because of the larger depth of charge insertion/extraction. The results confirm that magnetron sputtering technology provides a feasibility for electrochromic devices with excellent electrochromic performance.

Keywords: Magnetron Sputtering, Nickel Oxide, Electrochromism, Transmittance Modulation.

1. INTRODUCTION

Electrochromic materials exhibit reversible change in color and optical transmittance upon an electric voltage.[1,2] A typical electrochromic device has the potential applications in energy efficient eco architecture, mirrors, smart windows, and displays.[3,4] At present, inorganic electrochromic materials, such as WO$_3$ and NiO$_x$, have been widely investigated because of the good durability, large transmittance modulation, and low cost.[5–8] WO$_3$, as the most studied electrochromic material, has shown rather high efficiency for cathodic coloration and the mechanism of coloring and blenching is well understood.[9] For the purpose of further improving the transmittance modulation, it is necessary to research the anodic coloration material that present complementary coloration. A good candidate is Nickel oxide (NiO$_x$) that is a low cost material with

the advantages of good cyclic stability and high coloration efficiency.[10–13] However, the reason of the electrochromism is not settled that the absorption mechanism is poorly understood and the ionic species involved in the transmittance modulation are ambiguous.[14] Therefore, NiO$_x$ has attracted great attention in the last decades.

To realize the high performance of electrochromic device, there are several reports on NiO$_x$ films obtained by different chemical and physical deposition techniques.[15–20] Zhou et al. reported the electrochromic properties and cyclic durability of Li–Ti co-doped NiO$_x$ films were enhanced by sol–gel method.[21] Li and Ti doping deteriorate the symmetry of NiO$_x$ cubic phase, increase lattice disorder, and change the valence state of Ni in the films. Nanoporous NiO$_x$/V$_2$O$_5$ hybrid films had been successfully prepared by combining chemical bath deposition and electrochemical deposition methods.[22] Good cyclic stability, better transmittance modulation, and high coloration

efficiency were obtained. Although NiO_x fims prepared by chemical methods has the good electrochromic properties, it is not suitable for large scale commercial application due to the disadvantages of uniformity and small area. Among the physical routes, magnetron sputtering and thermal evaporation both have been widely used.[23–25] NiO_x films deposited by thermal evaporation had the large transmittance modulation and short coloring/blenching response time, however, the durability was less than 200 cycles without lost of transmittance modulation because of the loose structure.[26] On the other hand, magnetron sputtered NiO_x films had the large transmittance modulation and good cyclic stability but the long response time due to the compact structure.[27] Consequently, the aim of this work is to prepare the surface roughened NiO_x films by controlling the sputtering conditions which have the good electrochromic performance and little response time (unpublished results). Further on, the effect of thickness on the electrochromic properties was investigated.

In this paper, NiO_x films were deposited on ITO-coated glass by DC magnetron sputtering. The effects of thickness on structure, morphology, electrochemical properties and optical properties were studied and analyzed. The results show that the electrochromic behavior of NiO_x films largely depends on the thickness. The 500-nm-thick NiO_x film has the large transmittance modulation, good durability, and long response time.

2. EXPERIMENTAL DETAILS

Thin films of NiO_x were made at room temperature by DC magnetron sputtering. The substrates were 2.5×2.5 cm² ITO transparent conductive glass, their sheet resistances were 30 Ω/Sq. The target was a 7.62-cm-diameter plate of metallic nickel (99.995%), and the target-substrate separation was 10 cm. A mixture of argon (99.995%) and oxygen (99.995%) was used in the sputtering atmosphere, the ratio of the oxygen partial pressure was set at a constant value of 19%. The initial chamber pressure was 1.0×10^{-3} Pa, and the total pressure during sputtering was maintained at 0.3 Pa. The sputtering power was 100 W. The substrate was kept uniform rotation during the sputtering process in order to ensure the uniformity of NiO_x films.

The film thickness was determined by surface profilometry using a DektakXT instrument and the thicknesses were 100 nm, 200 nm, 300 nm, 400 nm and 500 nm, respectively. The structures were determined by X-ray diffraction (XRD) using a APEX II DUO. Jsm-6510 scanning electron microscope (SEM) and atomic force microscope (AFM) were used to study the surface morphology of NiO_x films. Visible light transmittance spectra of the films were studied by Lambda950. Electrochemical workstation was used to study the electrochemical properties of NiO_x films. The electrolytic cell was the standard three electrode system and immersed in 1 M $LiClO_4$-PC electrolyte solution, the counter electrode was a Pt foil, the reference electrode was Ag/AgCl, and the working electrode was the NiO_x film. The voltage range was −0.5 to 1.5 V versus Ag/AgCl, and the voltage sweep rate was 50 mV/s.

3. RESULTS AND DISCUSSION

Figure 1 shows the X-ray diffraction patterns of as-deposited NiO_x films. The films give the clear evidence that NiO_x films have the cubic fcc structure (JCDPS No. 47-1049). There has no preferred orientation observed in the films which indicates NiO_x films have a polycrystalline structure. Five diffraction peaks corresponding to (111), (200), (220), (311) and (222) planes are apparent, and peaks of impurity or other oxidation state of Ni are not found. The Scherrer's formula $D = 0.89\lambda/(\beta \cos\theta)$ is applied to determine the crystallite size of NiO_x films, where β is the full width at half-maximum of an X-ray diffraction peak and θ is the diffraction angle.[16] The crystallite sizes of 11.63 nm, 12.79 nm, 11.56 nm, 13.67 nm, and 13.72 nm are obtained for 100 nm, 200 nm, 300 nm, 400 nm, and 500 nm NiO_x films respectively from the (111) peak. The thick films have the large crystallite size suggesting an improvement of the crystallinity. It is worth noting that there is no diffraction peak that shows any higher oxides such as Ni_2O_3 or NiO_2, however, the color of the as-deposited films is dark brown indicating the appearance of Ni^{3+} ions in Ni_2O_3 configuration which exists in amorphous state. Because the Ni^{3+} ions act as the color centers in NiO_x films, the low transmittance of initial state films and the color of dark brown can prove the existence of Ni^{3+} ions. All the prepared NiO_x films have the Ni^{3+} and Ni^{2+} ions, which can result in the large transmittance modulation.[24]

Figure 2 presents the scanning electron microscopy (SEM) data for NiO_x films with the thicknesses of 100 to 500 nm. The surface features strongly depend on the thickness. NiO_x films with the thickness of 100 nm and 200 nm
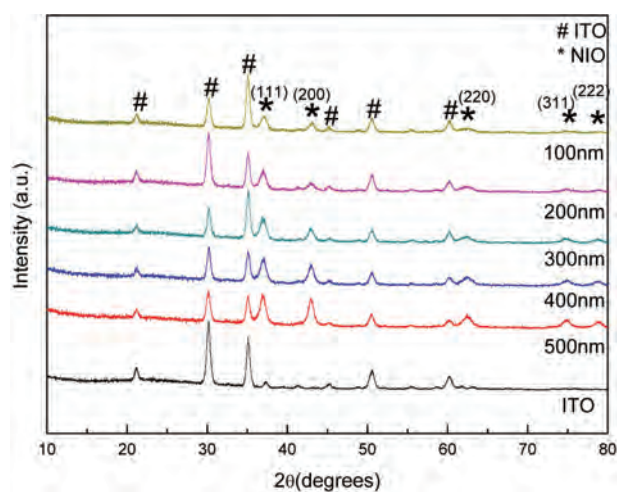

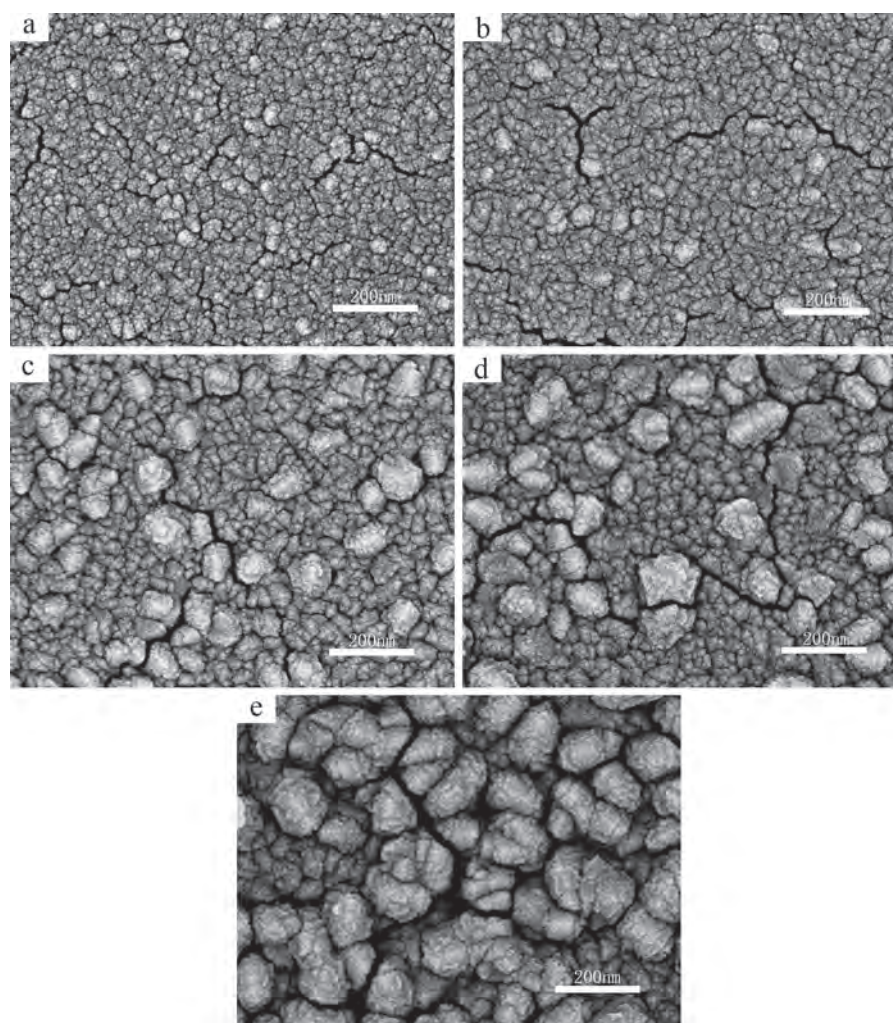**Figure 1.** XRD patterns of NiO_x films with different thickness.

Figure 2. SEM images of NiO$_x$ films with the thickness of (a) 100 nm, (b) 200 nm, (c) 300 nm, (d) 400 nm, and (e) 500 nm.

have the smooth, uniform surface, and small particle size. 300–500 nm thick NiO$_x$ films possess large particle size and porosity, and then the rough surface. It is indicated that less particles are found as the thickness increases implying to a certain extent the increase of crystallinity by combining the XRD results. Moreover, the rough surface and large porosity in NiO$_x$ films are beneficial for the insertion/extraction of Li$^+$ ions and electrons to obtain a good electrochemical performance.

The AFM topography of NiO$_x$ films are displayed in Figure 3. The roughness increases from 3.6 nm to 25 nm as the NiO$_x$ thickness increases (Fig. 3(f)), corroborating the SEM analysis.

Electrochemical properties of NiO$_x$ films are given in Figure 4 by cyclic voltammetry in an electrolyte of 1 M LiClO$_4$-PC. Two oxidative peaks at the voltages of 0.4 V and 1 V are apparent which shows the anodic oxidation of Ni^{2+} to Ni^{3+} and Ni^{4+} corresponding to the colored state.[22] Meanwhile, two reductive peaks appear at -0.1 V and 0.75 V and suggest the cathodic reduction of Ni^{3+} and Ni^{4+} to Ni^{2+} which corresponds to the

bleached state. A simple two-step electrochemical reaction scheme for Li$^+$ insertion/extraction was presented to illustrate the oxidation-reduction reaction.[23] It refers to an initial irreversible bleaching of as-deposited NiO$_x$ film, NiO$_x$+yLi$^+$+ye$^- \rightarrow$ Li$_y$NiO$_x$, where e$^-$ represents electrons, followed by a reversible reaction between bleached Li$_y$NiO$_x$ and colored Li$_{y-z}$NiO$_x$ as shown by Li$_y$NiO$_x \leftrightarrow$ Li$_{y-z}$NiO$_x$+zLi$^+$+ze$^-$. The full cycles show qualitatively similar C–V data after 20 cycles for each film which indicates NiO$_x$ films have the good cyclic durability. More importantly, both the anodic and cathodic currents increase which suggests that the amount of ions and electrons inserted into the films increases, implying the electrochemical activity of NiO$_x$ films is improved with increasing the thickness. Simultaneously, the charge density is enlarged as the thickness is increased (Figs. 4(a′)–(e′)). The thicker the NiO$_x$ film, the larger the depth of charge insertion/extraction, which means more amount of charge transfer takes place and leads to the excellent electrochemical properties. The diffusion coefficient D of Li$^+$ ions is calculated by using the Randles-Sevcik
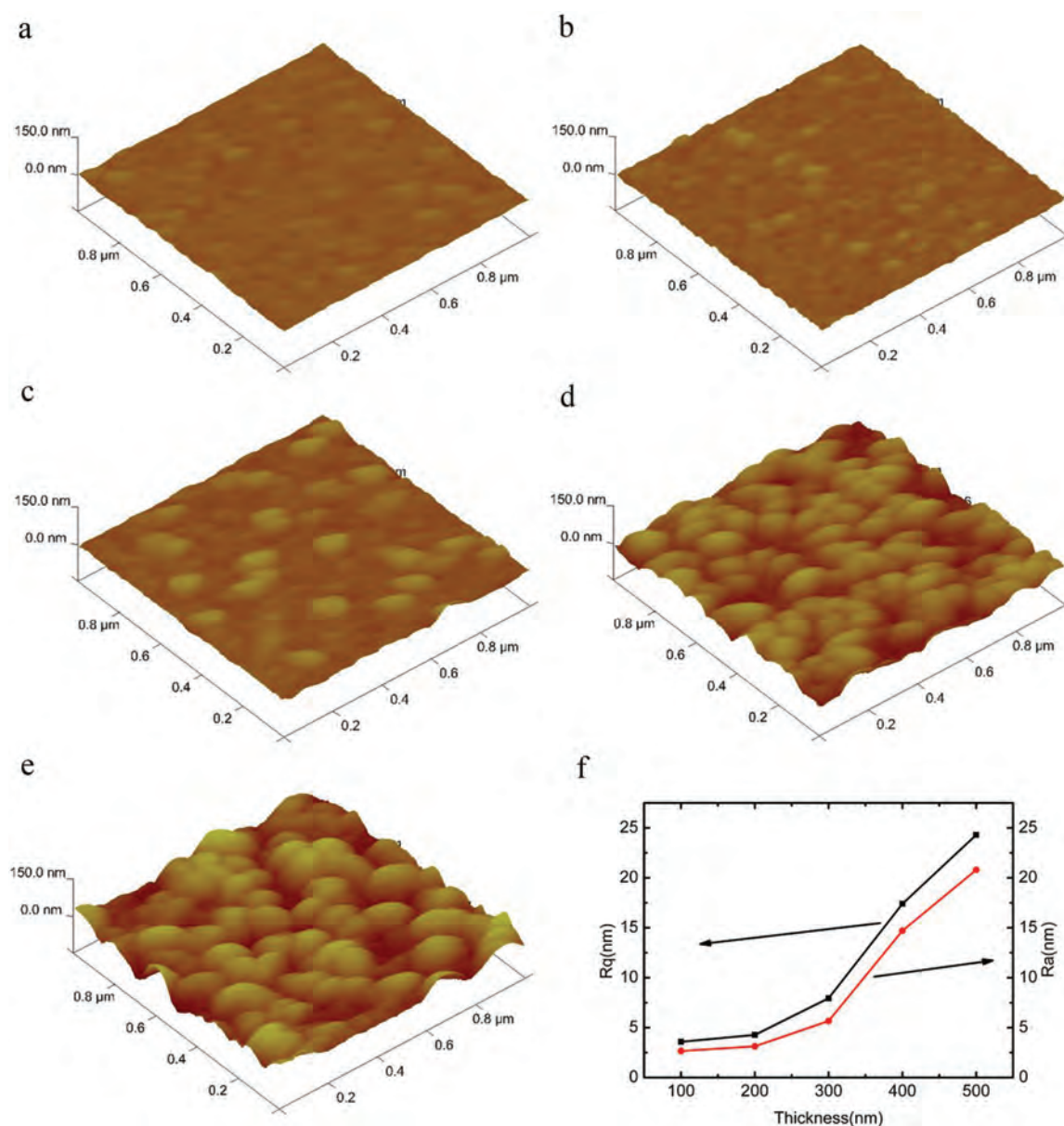
Figure 3. AFM images of NiO$_x$ films with the thickness of (a) 100 nm, (b) 200 nm, (c) 300 nm, (d) 400 nm, and (e) 500 nm. (f) Roughness of NiO$_x$ films as a function of thickness.

equation: $i_p = 2.69 \times 10^5 n^{3/2} A D^{1/2} C v^{1/2}$, where i_p is the peak current, n is the number of electrons participating in the electrochemical reaction which is normally 1, A is the area of electrode, D is the diffusion coefficient of Li$^+$ ions, C is the concentration of active ions in the electrolyte solution, v is the sweep rate.[28] The peak current is obtained from the cyclic voltammograms at the different sweep rate (not shown here). The anodic and cathodic diffusion coefficients for 200 nm NiO$_x$ film are 3.46×10^{-11} cm^{2}s^{-1} and 1.37×10^{-12} cm^{2}s^{-1} respectively, and are increased to the values of 1.98×10^{-10} cm^{2}s^{-1} and 2.49×10^{-10} cm^{2}s^{-1} for 500 nm NiO$_x$ film. On the other hand, the ionic conductivity (σ) was measured by using the Electrochemical Impedance Spectroscope (EIS). The ionic conductivity of

3.74×10^{-7} cm^{-2}s, 7.5×10^{-7} cm^{2}s, 1.17×10^{-6} cm^{2}s, 1.55×10^{-6} cm^{2}s, and 1.99×10^{-6} cm^{2}s are obtained for NiO$_x$ films with the thickness of 100 nm, 200 nm, 300 nm, 400 nm, and 500 nm, respectively. It is clear that the electrochemical activity is improved as the film thickness increases.

In order to evaluate the cyclic durability, cyclic voltammogram of 500-nm-thick NiO$_x$ film was performed by 500 cycles which shows the NiO$_x$ film has the good cyclic durability (seen in Fig. 5). Thus, the magnetron sputtered NiO$_x$ films have better cyclic durability than thermal evaporated films which have less than 200 cycles.[26] It can be attributed to the compact structure of NiO$_x$ film deposited by magnetron sputtering technology.
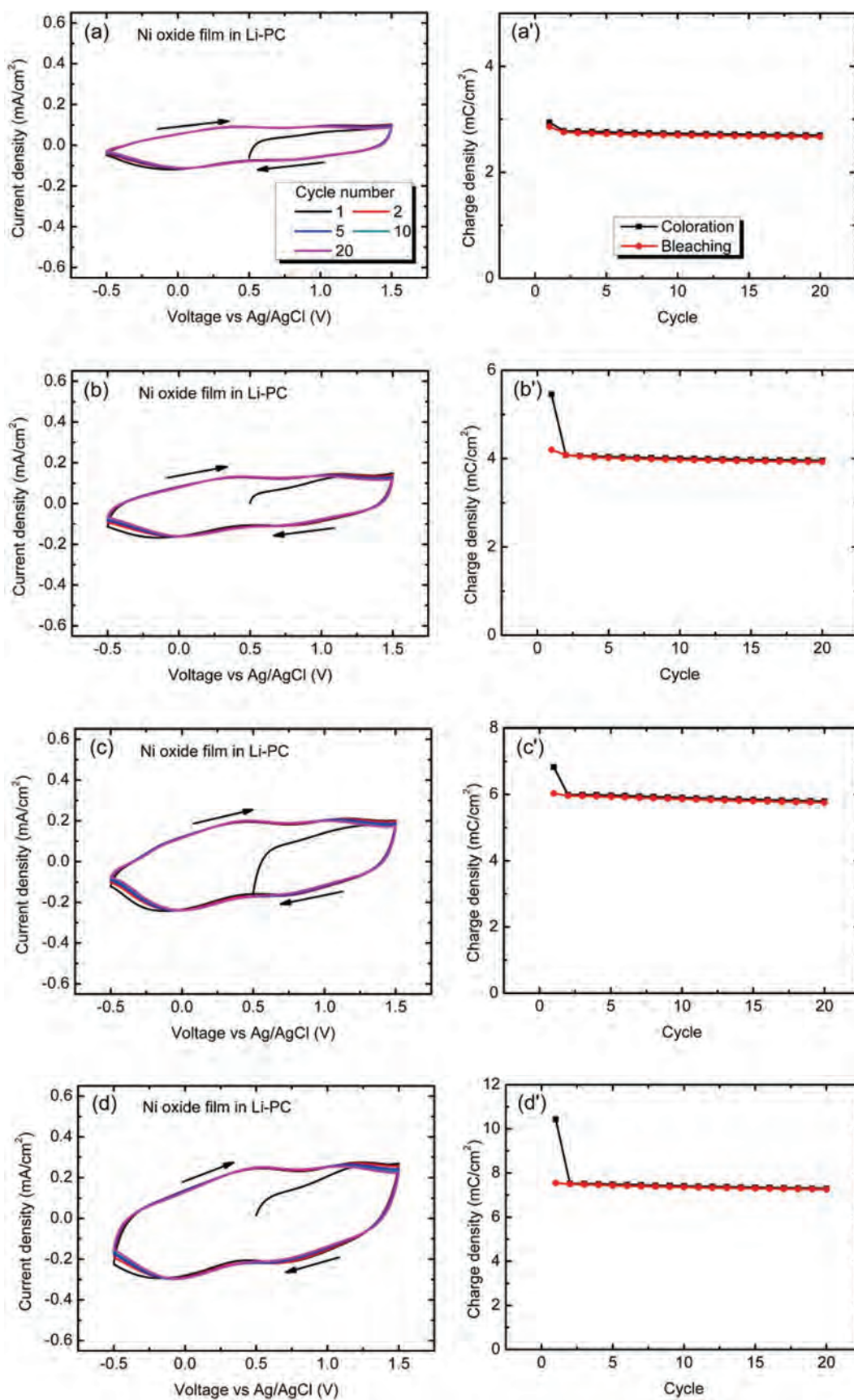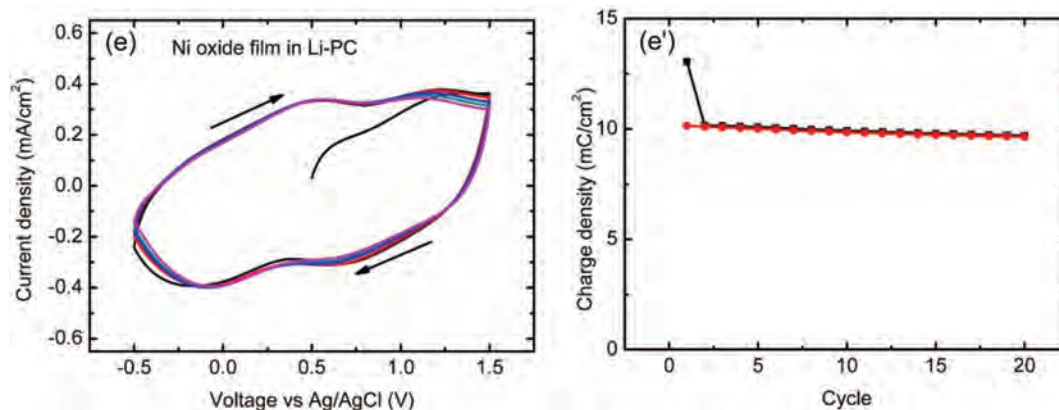
Figure 4. Continued.

Figure 4. Cyclic voltammograms of NiO$_x$ films with the thickness of (a) 100 nm, (b) 200 nm, (c) 300 nm, (d) 400 nm, and (e) 500 nm, immersed in 1 M LiClO$_4$-PC electrolyte. The voltage sweep rate was 50 mV/s and arrows denote sweep direction. (a′–e′) Charge densities obtained from CV data in (a–e).
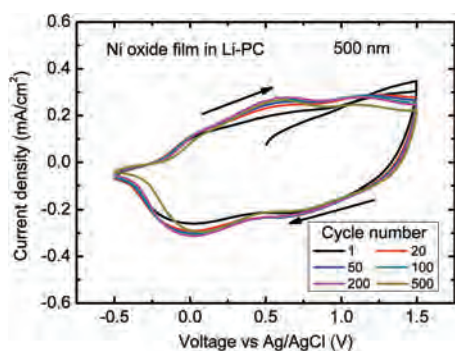

Figure 5. Cyclic voltammograms of the 500-nm-thick NiO$_x$ film in 1 M LiClO$_4$-PC electrolyte. The voltage sweep rate was 50 mV/s and arrows denote sweep direction.

Figure 6 reports the spetral transmittance of NiO$_x$ films in initial state, colored state, and bleached state. The transmittances of colored state and bleached state were measured by applying ±2 V in 1 M LiClO$_4$-PC electrolyte.

Table I. Color efficiency of NiO$_x$ films with different thickness.

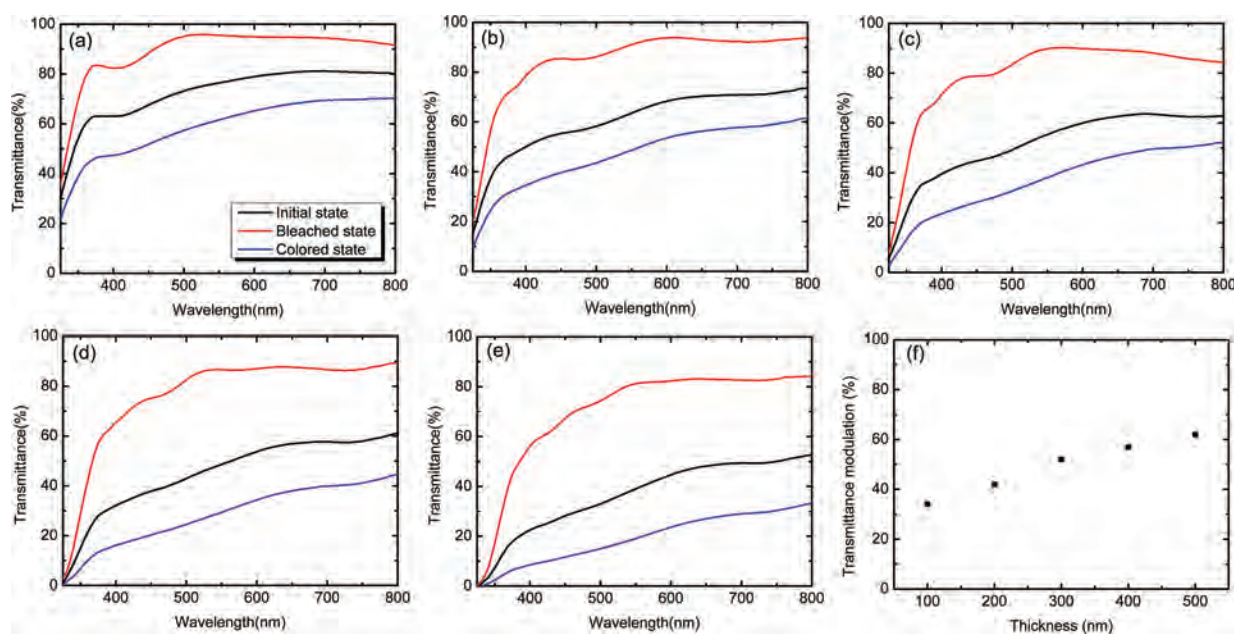| Film thickness (nm)	Transmittance (T_b) at 550 nm	Transmittance (T_c) at 550 nm	ΔT (%)	Optical density (ΔOD)	Color efficiency (cm^{2}C^{-1})
100	96	62	34	0.19	69.5
200	91	49	42	0.27	67.4
300	90	38	52	0.37	62.7
400	87	29	58	0.48	64.8
500	81	19	62	0.63	63.5

Figure 6. Spectral transmittance of NiO$_x$ films with the thickness of (a) 100 nm, (b) 200 nm, (c) 300 nm, (d) 400 nm, and (e) 500 nm, in 1 M LiClO$_4$-PC. The voltages of bleached state and colored state are −2 V and 2 V, respectively. (f) Transmittance modulation of NiO$_x$ films at the wavelength of 550 nm.
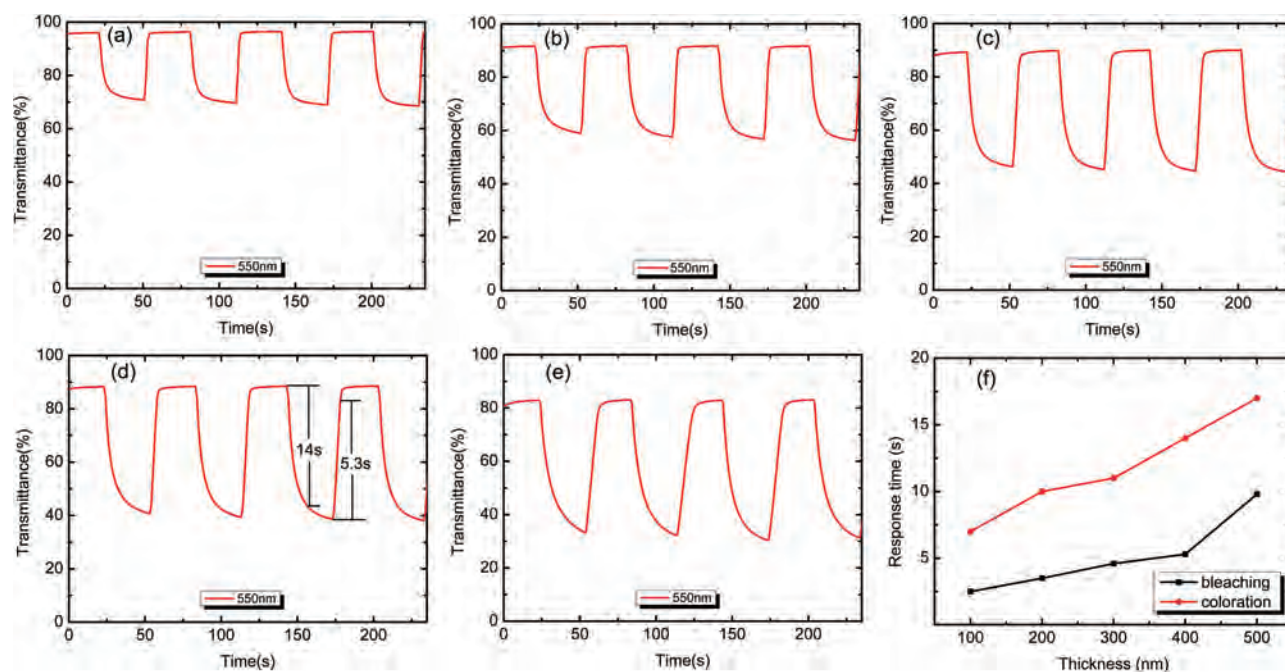
Figure 7. Lifetime cycle measurements of NiO$_x$ films with the thickness of (a) 100 nm, (b) 200 nm, (c) 300 nm, (d) 400 nm, and (e) 500 nm. (f) Coloring and bleaching response times obtained from the data of (a–e).

The transmittance of initial state lies modestly between the colored state and bleached state which shows a good proportion of Ni^{2+} to Ni^{3+}. It can be expected that the transmittance of initial state at 550 nm decreases with the increase of thickness. The transmittance modulation defined as the difference of transmittance between the colored state and bleached state at 550 nm increases as the thickness increases, being 34%, 42%, 52%, 58%, and 62% for the NiO$_x$ films of 100 nm, 200 nm, 300 nm, 400 nm, and 500 nm respectively. It can be explained that the thicker NiO$_x$ film has the larger roughness and porosity (seen from the SEM and AFM results) which are in favor of the insertion/extraction of ions and electrons and result in the large transmittance modulation. The color efficiency (CE), which is defined as the difference in optical density per amount of charge exchange (ΔQ), is given by the following equations: $CE = (\Delta OD/\Delta Q)_{\lambda=550\,nm}$ and $\Delta OD = (\log T_b/T_c)_{\lambda=550\,nm}$, where T_b and T_c are the transmittance of the films in the bleached state and colored state respectively at the wavelength of 550 nm, ΔOD is the optical density. The values of color efficiency for NiO$_x$ films are presented in Table I. The high color efficiencies of more than 62 cm^{2}C^{-1} are obtained in NiO$_x$ films which are larger than the other experimental results.[16, 24, 26]

Figure 7 shows the coloring and bleaching response time obtained from the lifetime cycle measurement for NiO$_x$ films. Coloring and bleaching response times are defined as the time required for 90% changes in the entire transmittance modulation. Simply speaking, the transmittances of bleached state and colored state are 88.5% and 38.7% respectively for 400 nm NiO$_x$ film at the wavelength

of 550 nm. The transmittance modulation is 49.8% and the 90% change is 44.8%. Accordingly, the coloring and bleaching response times are the time as the transmittances of bleached and colored state change from 88.5% to 43.7% and from 38.7% to 83.5%, respectively. So the coloring and bleaching response times are 14 s and 5.3 s for 400 nm NiO$_x$ film, respectively. Generally, the coloring response times are 7 s, 10 s, 11 s, 14 s, and 17 s, while the bleaching response times are 2.5 s, 3.5 s, 4.6 s, 5.3 s, and 9.8 s for NiO$_x$ films with the thickness of 100 nm, 200 nm, 300 nm, 400 nm, and 500 nm respectively. It is concluded that the coloring or bleaching response time enlarges with thickness because of the more rough surface and larger porosity of NiO$_x$ film. Therefore, larger number of Li$^+$ ions participating in the oxidation-reduction reaction and larger depth of charge insertion/extraction spend more time. The coloring and bleaching response times of 17 s and 9.8 s are acceptable for 500 nm NiO$_x$ film, however, they can be further decreased by ion-doping.

4. CONCLUSIONS

Nickel oxide (NiO$_x$) films with different thickness were prepared by DC magnetron sputtering at room temperature. The effect of thickness on the electrochromic properties was investigated. The observations show that the structure, morphology, electrochemical properties, and transmittance modulation are largely dependent on the thickness. The NiO$_x$ film has the larger roughness and porosity as the thickness increases, which results in the good electrochemical stability and large transmittance modulation, but the acceptable coloring/bleaching

response time. Therefore, the results confirm that magnetron sputtering technology provides a feasibility for electrochromic devices with excellent electrochromic performance.

References and Notes

1. B. D. R. Rosseinsky and R. J. Mortimer, *Adv. Mater.* 13, 783 (**2001**).
2. V. K. Thakur, G. Q. Ding, J. Ma, P. S. Lee, and X. H. Lu, *Adv. Mater.* 24, 4071 (**2012**).
3. C. G. Granqvist, Handbook of Inorganic Electrochromic Materials, Elsevier Science B. B. V., Amsterdam (**1995**).
4. C. G. Granqvist, Handbook of Electrocemistry, CRC Press, Boca Raton (**1997**), p. 587.
5. E. Eren, G. Y. Karaca, U. Koc, L. Oksuz, and A. U. Oksuz, *Thin Solid Films* 634, 40 (**2017**).
6. D. S. Hong, W. X. Wang, Y. S. Chen, J. R. Sun, and B. G. Shen, *Appl. Phys. Lett.* 105, 113504 (**2014**).
7. H. Moulki, D. H. Park, B. K. Min, H. Kwon, S. J. Hwang, J. H. Choy, T. Toupance, G. Campet, and A. Rougier, *Electrochim. Acta* 74, 46 (**2012**).
8. K. K. Purushothaman and G. Muralidhran, *Sol. Energy Mater. Sol. Cells* 93, 1195 (**2009**).
9. G. A. Niklasson and C. G. Granqvist, *J. Mater. Chem.* 17, 127 (**2007**).
10. R. T. Wen, C. G. Granqvist, and G. A. Niklasson, *Appl. Phys. Lett.* 105, 163502 (**2014**).
11. X. C. Lou, X. J. Zhao, and X. He, *Sol. Energy* 83, 2103 (**2009**).
12. J. Denayer, G. Bister, P. Simonis, P. Colson, A. Maho, P. Aubry, B. Vertruyen, C. Henrist, V. Lardot, F. Cambier, and R. Cloots, *Appl. Surf. Sci.* 321, 61 (**2014**).
13. X. Y. Qi, G. Su, G. S. Bo, L. X. Cao, and W. Liu, *Surf. Coat. Tech.* 272, 79 (**2015**).
14. J. S. E. M. Svensson and C. G. Granqvist, *Appl. Phys. Lett.* 49, 1566 (**1986**).
15. H. J. Ahn, H. S. Shim, Y. S. Kim, C. Y. Kim, and T. Y. Seong, *Electrochem. Commun.* 7, 567 (**2015**).
16. R. T. Wen, G. A. Niklasson, and C. G. Granqvist, *Thin Solid Films* 565, 128 (**2014**).
17. Y. Ren, W. K. Chim, L. Guo, H. Tanoto, J. S. Pan, and S. Y. Chiam, *Sol. Energy Mater. Sol. Cells* 116, 83 (**2013**).
18. H. Huang, J. Tian, W. K. Zhang, Y. P. Gan, X. Y. Tao, X. H. Xia, and J. P. Tu, *Electrochim. Acta* 56, 4281 (**2011**).
19. K. Zhang, X. Q. Zhang, C. X. Zhang, S. J. Zhang, X. C. Wang, D. L. Sun, and M. A. Aegerter, *Sol. Energy Mater. Sol. Cells* 114, 192 (**2013**).
20. G. F. Cai, X. Wang, M. Q. Cui, P. Darmawan, J. X. Wang, A. L. S. Eh, and P. S. Lee, *Nano Energy* 12, 258 (**2015**).
21. J. L. Zhou, G. Luo, Y. X. Wei, J. M. Zheng, and C. Y. Xu, *Electrochim. Acta* 186, 182 (**2015**).
22. Y. N. Liu, C. Y. Jia, Z. Q. Wan, X. L. Weng, J. L. Xie, and L. J. Deng, *Sol. Energy Mater. Sol. Cells* 132, 467 (**2015**).
23. R. T. Wen, C. G. Granqvist, and G. A. Niklasson, *Adv. Funct. Mater.* 25, 3359 (**2015**).
24. D. M. Dong, W. W. Wang, G. B. Dong, Y. L. Zhou, Z. H. Wu, M. Wang, F. M. Liu, and X. G. Diao, *Appl. Surf. Sci.* 357, 799 (**2015**).
25. I. Porqueras and E. Bertran, *Thin Solid Films* 398, 41 (**2001**).
26. S. Pereira, A. Goncalves, N. Correia, J. Pinto, L. Pereira, R. Martins, and E. Fortunato, *Sol. Energy Mater. Sol. Cells* 120, 109 (**2014**).
27. X. W Song, G. B. Dong, F. Y. Gao, Y. Xiao, Q. R. Liu, and X. G. Diao, *Vacuum* 111, 48 (**2015**).
28. K. S. Usha, R. Sivakumar, C. Sanjeeviraja, V. Sathe, V. Ganesan, and T. Y. Wang, *RSC Adv.* 6, 79668 (**2016**).